

## Triple- $\vec{q}$ Octupolar Ordering in NpO<sub>2</sub>

J. A. Paixão,<sup>1</sup> C. Detlefs,<sup>2</sup> M. J. Longfield,<sup>3</sup> R. Caciuffo,<sup>4</sup> P. Santini,<sup>5,\*</sup> N. Bernhoeft,<sup>6</sup> J. Rebizant,<sup>3</sup> and G. H. Lander<sup>3</sup>

<sup>1</sup>*Departamento de Física, Universidade de Coimbra, P-3004 516 Coimbra, Portugal*

<sup>2</sup>*European Synchrotron Radiation Facility, Boîte Postale 220, F-38043 Grenoble Cedex, France*

<sup>3</sup>*European Commission, Joint Research Centre, Institute for Transuranium Elements, Postfach 2340, D-76125 Karlsruhe, Germany*

<sup>4</sup>*Istituto Nazionale per la Fisica della Materia, Dipartimento di Fisica ed Ingegneria dei Materiali, Università di Ancona, Via Breccie Bianche, I-60131 Ancona, Italy*

<sup>5</sup>*Oxford Physics, Clarendon Laboratory, Oxford OXI 3PU, United Kingdom*

<sup>6</sup>*Département de Recherche Fondamentale sur la Matière Condensée, Commissariat à l'Énergie Atomique-Grenoble, F-38054 Grenoble, France*

(Received 30 April 2002; published 15 October 2002)

We report the results of resonant x-ray scattering experiments performed at the Np  $M_{4,5}$  edges in NpO<sub>2</sub>. Below  $T_0 = 25$  K, the development of long-range order of Np electric quadrupoles is revealed by the growth of superlattice Bragg peaks. The polarization and azimuthal dependence of the intensity of the resonant peaks are well reproduced assuming anisotropic tensor susceptibility scattering from a triple- $\vec{q}$  longitudinal antiferroquadrupolar structure. Electric-quadrupole order in NpO<sub>2</sub> could be driven by the ordering at  $T_0$  of magnetic octupoles of  $\Gamma_5$  symmetry, splitting the Np ground state quartet and leading to a singlet ground state with zero dipole-magnetic moment.

DOI: 10.1103/PhysRevLett.89.187202

PACS numbers: 75.25.+z, 75.10.-b

For half a century the low temperature properties of NpO<sub>2</sub> have mystified theorists and experimentalists alike. Upon cooling from room temperature a *single* phase transition is observed at  $T_0 \approx 25.5$  K [1]. Similarities with UO<sub>2</sub> [2] suggested a magnetic nature of the phase transition, but no magnetic order was found by neutron diffraction [3] or by Mößbauer spectroscopy [4], which established an upper limit of  $\approx 0.01\mu_B$  for the *ordered* magnetic moment  $\vec{\mu}_{\text{ord}}$ . However, Np<sup>4+</sup> ions in NpO<sub>2</sub> are Kramers ions ( $5f^3, {}^4I_{9/2}$ ). In the absence of interactions breaking time-reversal symmetry the ground state has to carry a magnetic moment,  $\vec{\mu}$ , whatever the crystalline environment. A fluctuating magnetic moment of finite size would be revealed by a Curie-like divergence of the susceptibility at low temperatures, whereas the experiments reveal a flat susceptibility between 15 and 5 K [5]. Moreover, no evidence for a crystallographic distortion, neither external nor internal, has been found by synchrotron experiments [6].

Another element of the puzzle was recently provided by muon spin relaxation ( $\mu$ SR) experiments, showing the abrupt appearance of a precession signal below  $T_0$  [7]. This implies that the order parameter (OP) sets up a magnetic field at the muon stopping site and provides definitive evidence that the OP breaks invariance under time reversal. By assuming antiferromagnetic (AF) order of the same kind of that established for UO<sub>2</sub>, i.e., a type-I, triple- $\vec{q}$  structure, the authors deduced an ordered moment  $\mu_{\text{ord}} \approx 0.1\mu_B$ , a value much larger than the upper limit compatible with Mößbauer spectroscopy. In parallel with this finding, direct evidence for long-range order in NpO<sub>2</sub> was obtained through the observation below  $T_0$  of superlattice reflections in resonant x-ray scattering (RXS) experiments at the Np  $M_{4,5}$  absorption edges [6]. The su-

perstructure Bragg peaks occur at  $\vec{Q} = \vec{G} + \langle 001 \rangle$  positions, where  $\vec{G}$  is a reciprocal lattice vector. This is the same periodicity found for the AF phase in UO<sub>2</sub>, and the observations were taken as evidence for the occurrence of longitudinal triple- $\vec{q}$  AF order. Santini and Amoretti [8] pointed out the possibility of explaining the whole body of experimental evidence assuming magnetic-octupole order instead of magnetic-dipole order. Octupolar order would lift the degeneracy of the  $\Gamma_8$  Np ground state and generate an interstitial magnetic field, in agreement with neutron spectroscopy [9] and muon spin resonance results. However, octupolar order can be directly observed in RXS only through  $E2$  resonances, while the resonances observed in [6] are at the  $E1$  absorption edge. Indeed, all previous experimental data taken at the actinide  $M_{4,5}$  edges indicate a very strong dominance of  $E1$  processes ( $3d_{3/2,5/2} \leftrightarrow 5f$ ). To our knowledge there is no evidence for  $E2$  contributions ( $3d_{3/2,5/2} \leftrightarrow 6g$ ), and indeed matrix elements involving  $E2$  promotion to  $6g$  states are expected to be too small to allow for any observable signal.

To clarify the above confusion, we have undertaken a new RXS experiment at the magnetic scattering beam line, ID20, of the European Synchrotron Radiation Facility (ESRF). We performed polarization analysis (PA) of the diffracted radiation and measured the dependence of the intensity from the azimuthal angle,  $\psi$  (the angle describing the rotation of the crystal about the scattering vector). These analyses were not possible in the experiment reported earlier in [6], preventing an unambiguous determination of the origin of the resonance. Indeed, the results we present in this Letter show that the superlattice peaks in NpO<sub>2</sub> are not magnetic but arise from the asphericity of the Np  $5f$  electron density leading to an anomalous tensor component in the atomic

scattering factor. In other words, the superlattice peaks signal the occurrence of electric-quadrupole long-range order below  $T_0$ . This conclusion is incompatible with the particular octupolar model given in Ref. [8], which predicts an undistorted charge density for the  $5f$  ground state, with vanishing quadrupole moment.

The experiment was performed on a single crystal of  $0.7 \times 0.7 \times 0.2$  mm<sup>3</sup> in volume, with a flat (001) surface. A closed-cycle refrigerator equipped with an azimuthal-rotation stage provided a base temperature of 12 K. An Au(111) single crystal was used to analyze whether the polarization of the scattered beam was parallel ( $\pi$ ) or perpendicular ( $\sigma$ ) to the scattering plane. The incident beam had  $\sigma$  polarization and the scattering plane was vertical.

Figure 1 shows the  $\sigma \rightarrow \pi$  intensity of the  $\vec{Q} = (003)$  superlattice reflection as a function of the photon energy,  $E$ , around the Np  $M_4$  absorption edge. The data can be fit to a Lorentzian-squared line shape, centered near the  $E1$  threshold. The presence of a resonance in the  $\sigma \rightarrow \sigma$  channel (not shown) excludes that the scattering arises from dipole-magnetic order, as this would give only  $\sigma \rightarrow \pi$  resonant scattering. Studies measuring magnetic order at actinide  $M$  edges have shown Lorentzian energy profiles, whereas we clearly observe a Lorentzian-squared form, as is expected when the intermediate state splitting is much smaller than the core hole lifetime [10].

The results of  $\psi$  (azimuthal) scans about the (003) peak, taken at  $T = 12$  K with  $E = 3.846$  keV, are shown in Fig. 2(a) for both the  $\sigma \rightarrow \sigma$  and the  $\sigma \rightarrow \pi$  channel. Figures 2(b) and 2(c) show, respectively, the  $\psi$  dependence of the Stokes parameter  $P_1 = (I_{\sigma \rightarrow \sigma} - I_{\sigma \rightarrow \pi}) / (I_{\sigma \rightarrow \sigma} + I_{\sigma \rightarrow \pi})$  and  $P_2 = (I_+ - I_-) / (I_+ + I_-)$  [11], for the (001) and (003) reflections.  $P_2$  can be considered

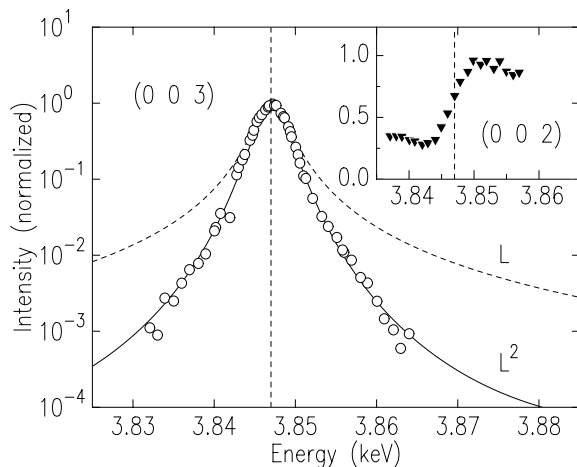


FIG. 1. Energy scans through the Np  $M_4$  absorption edge. The  $\sigma \rightarrow \pi$  (main panel) and  $\sigma \rightarrow \sigma$  (not shown) resonances of the (003) superstructure peak have a Lorentzian-squared (solid line) rather than a Lorentzian (dashed line) line shape. The maximum at the resonance lies at the absorption edge as measured at the (002) Bragg reflection (inset).

as a measure of the phase relation between the two polarization channels and is defined by the intensities measured with the analyzer oriented at  $\pm 45^\circ$  with respect to the scattering plane,

$$I_{\pm} \propto \frac{1}{\sqrt{2}} |F_{\sigma \rightarrow \sigma} \pm F_{\sigma \rightarrow \pi}|^2, \quad (1)$$

where  $F_{\sigma \rightarrow \sigma}$  and  $F_{\sigma \rightarrow \pi}$  are the  $\sigma \rightarrow \sigma$  and  $\sigma \rightarrow \pi$  scattering amplitudes.

The dependence of polarization and intensity of the scattered radiation on  $\psi$  can be modeled with satisfactory agreement by assuming a triple- $\vec{q}$  antiferroquadrupolar ordering of ( $\Gamma_5$ ) quadrupoles, and using the anisotropic tensor susceptibility (ATS) cross section [12–14] as detailed below and shown by the lines drawn in Fig. 2.

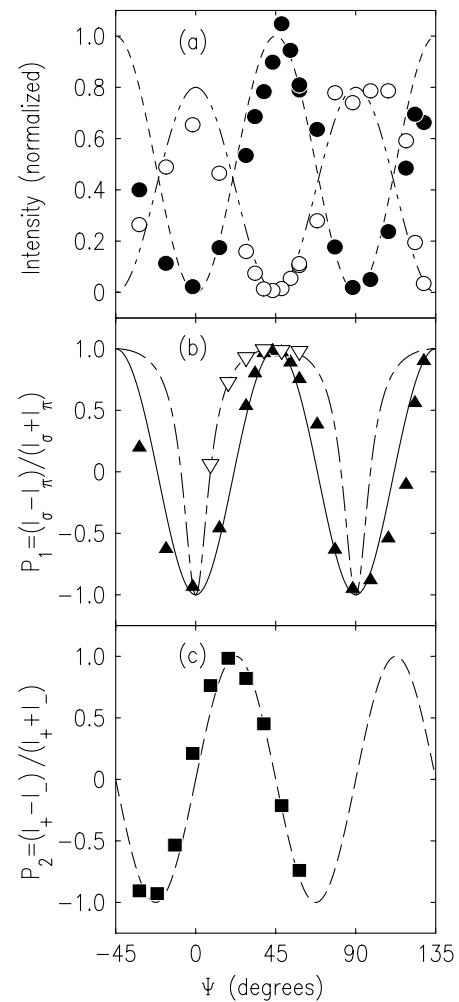


FIG. 2. Dependence of the scattering on the azimuthal angle,  $\psi$ : (a) intensity at the (003) quadrupolar reflection in the  $\sigma$  (filled circles) and  $\pi$  (open circles) channels with incident polarization  $\sigma$ . Different scaling factors have been applied to correct for differences in the efficiency of the PA in the  $\sigma$  and  $\pi$  settings. (b) Stokes parameter  $P_1$  for the (001) (open triangles) and (003) (filled triangles) quadrupolar reflections. (c) Stokes parameter  $P_2$  for the (003) peak. The lines represent model calculations based on Eqs. (1)–(4).

Above  $T_0$ ,  $\text{NpO}_2$  crystallizes in the fluorite structure with space group (SG)  $Fm\bar{3}m$ ,  $\text{Np}^{4+}$  at  $4a$  and  $\text{O}^{2-}$  ions at  $8c$  Wyckoff positions. A periodic distribution of electric quadrupoles can be Fourier expanded, whatever the type of order. A triple- $\vec{q}$  structure is obtained when three components of the star of the propagation vector  $\vec{q}$  enter in the Fourier sum. For  $\vec{q}_1 = (100)$ ,  $\vec{q}_2 = (010)$ , and  $\vec{q}_3 = (001)$ , the arrangement schematically shown in Fig. 3 is obtained, with charge distribution distorted along the  $\langle 111 \rangle$  directions of the cubic unit cell. The SG symmetry is lowered from  $Fm\bar{3}m$  to  $Pn\bar{3}m$ , the only maximal nonisomorphic subgroup of  $Fm\bar{3}m$  that is non-symmorphic and simple cubic. Within this SG, Np ions can be accommodated on the  $4b$  positions, with reduced point symmetry  $D_{3d}$  but the same crystallographic extinction rules of the FCC paraquadrupolar SG. Oxygen ions can occupy two inequivalent positions ( $2a$  and  $6d$ ), where all coordinates are *uniquely fixed by symmetry alone*, so that this electronic phase transition does not allow a shift of the oxygen ions. The symmetry of the ordered state remains cubic and, apart from a possible change of the lattice parameter [6], the transition will not be accompanied by any distortion. In that case, the quadrupolar OP *cannot* be measured with neutron or *conventional* x-ray diffraction techniques.

RXS from quadrupolar order has recently been observed in several systems [15,16]. It is well described within the framework of ATS scattering [12–14], which occurs when the photon energy is tuned to an absorption edge of an atom. The anisotropy of this atom's polarizability may lead to a finite scattering cross section at reflections which are normally forbidden due to glide plane or screw axis extinction rules. The scattering amplitude arising from  $E1$  transitions can be described by

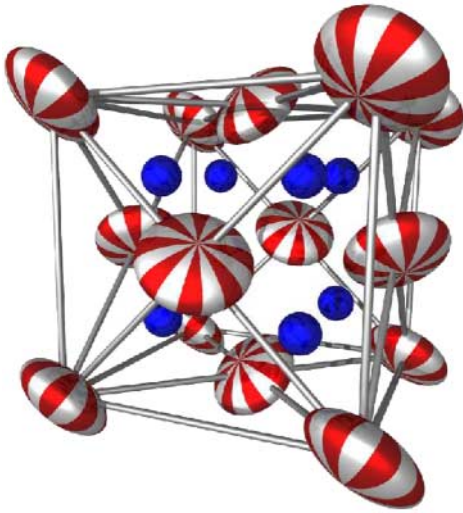


FIG. 3 (color online). Crystal structure of  $\text{NpO}_2$  in the anti-ferroquadrupolar state with space group  $Pn\bar{3}m$ . The ellipsoids represent the orientation of the local symmetry axis at the Np position, not the actual charge distributions. The O atoms are shown as spheres.

second rank tensors, which are invariant under the point symmetry of the scattering atom.

The scattering amplitude for the induced quadrupolar order must be represented by a symmetric tensor  $\tilde{f}(\vec{Q})$ . For  $\vec{Q} = (00L)$ , with  $L$  odd, the scattering length is given by  $F(\vec{Q}) = \vec{\epsilon}' \cdot \tilde{f}(\vec{Q}) \cdot \vec{\epsilon} = \tilde{\Phi}(\epsilon'_x \epsilon_y + \epsilon'_y \epsilon_x)$ , where  $\vec{\epsilon}$  and  $\vec{\epsilon}'$  are the polarization vectors of the incident and scattered beam, and  $\tilde{\Phi}$  is proportional to the Fourier component of the quadrupolar operator,  $\Phi$ . With incident  $\sigma$  polarization and  $\vec{h}_0 = (100)$  as azimuthal reference vector, we find

$$F_{\sigma \rightarrow \sigma} = \tilde{\Phi} \sin(2\psi), \quad (2)$$

$$F_{\sigma \rightarrow \pi} = \tilde{\Phi} \sin(\theta) \cos(2\psi), \quad (3)$$

where  $\theta$  is the Bragg angle. The resulting scattered intensities are  $I_{\sigma \rightarrow \sigma} \propto |F_{\sigma \rightarrow \sigma}|^2$  and  $I_{\sigma \rightarrow \pi} \propto |F_{\sigma \rightarrow \pi}|^2$ . As shown in Fig. 2(a), the experimental data are well matched by this model with one overall scale factor. This factor can be eliminated by calculating the Stokes parameter  $P_1$ . The data are shown in Fig. 2(b), along with model calculations.

The quantities  $I_{\pm}$  defined in Eq. (1) are given by

$$I_{\pm} \propto |\tilde{\Phi}|^2 [1 - \cos^2(\theta) \cos^2(2\psi) \pm \sin(\theta) \sin(4\psi)]. \quad (4)$$

The Stokes parameter  $P_2$  can be calculated and is in good agreement with the experiments [Fig. 2(c)].

However, the quadrupolar order *alone* is not a sufficient ingredient, as it cannot explain the absence of a disordered magnetic moment [5] and the breaking of invariance under time reversal [7]. The lowest-rank multipolar OP consistent with the experimental findings (no ordered or fluctuating dipoles, broken time-reversal symmetry) is an *octupole* [8]. Under octahedral symmetry, the seven octupolar operators belong to irreducible representations  $\Gamma_2$ ,  $\Gamma_4$ , or  $\Gamma_5$ . A  $\Gamma_4$ -octupole OP must be ruled out. In fact, this would always be accompanied by an ordering of dipoles as the latter belong to  $\Gamma_4$  as well. A  $\Gamma_2$  OP is consistent with most properties of  $\text{NpO}_2$  [8], but it cannot explain the RXS results, as it does not carry an electric-quadrupole moment and the  $\sigma \rightarrow \sigma$  signal would vanish [17].  $\Gamma_5$  octupolar operators are given by symmetrized combinations of  $O_i = J_i(J_j^2 - J_k^2)$ , where  $ijk = xyz, yzx$ , or  $zxy$ . The little cogroup of the ordering wave vector is  $D_{4h}$ .  $\Gamma_5$  decomposes into the tetragonal representations  $\Gamma_4^{(t)}$  (1D) and  $\Gamma_5^{(t)}$  (2D), which identify two possible type-I octupolar orders, a “longitudinal” one and a “transverse” one. For a single- $\vec{q}$  structure, both types of OPs are inconsistent with the observed quenching of dipoles and with the present RXS results. There is just one single type of order which can explain all observations, and this is a triple- $\vec{q}$  longitudinal structure, in which the  $\Gamma_4^{(t)}$  OPs associated with the three wave vectors of the star of  $\vec{q}$  have the same amplitude,  $\rho$ . The simplest conceivable mean-field (MF) Hamiltonian for each of the four sublattices  $s$  includes the crystal field (CF) potential [8] and a

self-consistent octupolar interaction term

$$\lambda O[\vec{n}(s)]\langle O[\vec{n}(s)]\rangle(T), \quad (5)$$

where  $\vec{n}(s)$  represents one of the four inequivalent  $\langle 111 \rangle$  directions,  $O[\vec{n}(s)] = \sum_{l=x,y,z} O_l n_l(s)$ ,  $\lambda$  is a MF constant, and  $\langle O[\vec{n}(s)]\rangle(T)$  is the self-consistent average value of  $O[\vec{n}(s)]$ , which does not depend on  $s$  and is nonzero for  $T < T_0$ . The MF potential lowers the symmetry of the Np Hamiltonian from  $O_h$  to  $D_{3d}$  and splits the  $\Gamma_8$ -quartet CF ground state into two singlets,  $\Gamma_5$  and  $\Gamma_6$ , and one doublet,  $\Gamma_4$ , of  $D_{3d}$ .  $\Gamma_5$  and  $\Gamma_6$  are complex-conjugate representations, which are degenerate for a time-reversal invariant Hamiltonian, whereas their degeneracy is lifted by the time-odd OP. By choosing the value of  $\lambda$  which reproduces the observed  $T_0$ , the level sequence at  $T = 0$  is found to be singlet-doublet-singlet. The ground state has zero dipole moment and the susceptibility saturates for  $T \rightarrow 0$ , as observed [5]. These properties do not depend on the details of the CF Hamiltonian (i.e., on the precise value of the CF parameter  $x$  or whether  $J$  mixing is taken into account).

This octupolar OP induces the observed triple- $\vec{q}$  structure of  $\Gamma_5$  quadrupoles as secondary OP, with an amplitude  $\propto \rho^2$  in MF near  $T_0$ . The charge density is distorted along  $\vec{n}(s)$ , as quantified by the quadrupolar operator along  $\vec{n}(s)$ ,  $\Phi[\vec{n}(s)] \propto \alpha \{3[\vec{n}(s) \cdot \vec{J}]^2 - J(J+1)\}$ , where  $\alpha$  is a Stevens coefficient.  $\Phi$  is negative in the ordered phase, indicating a charge distribution ‘‘oblate’’ along  $\vec{n}(s)$ . This quadrupolar secondary OP is the quantity observed in the RXS experiment.

The model we propose excludes a lattice distortion or a shift of the oxygen positions. The reduction of the local symmetry at the Np site leads to an electric field gradient along the  $\langle 111 \rangle$  directions. This explains the line broadening observed below  $T_0$  in Mößbauer spectroscopy [4]. The octupolar order breaks time-reversal symmetry and thus allows the occurrence of interstitial magnetic fields as evidenced by  $\mu$ SR [7].

Finally, we remind the reader that we have *inferred* the triple- $\vec{q}$  symmetry and octupolar order from the boundary conditions set out by previous experimental observations, such as the absence of lattice distortions, the analogy to  $\text{UO}_2$ , and from the excellent agreement of our data with the model. At the  $E2$  edge, the principal OP, i.e., the  $\Gamma_5$  magnetic octupole, is expected to give a resonant contribution to the scattered intensity [17], comparable to that expected at the same energy from the secondary OP, the  $\Gamma_5$  electric quadrupoles. However, no signal has been detected at the  $E2$  edge, indicating that both contributions are below the sensitivity of the experimental device we used. At the  $E1$  edge the intensity is almost entirely of quadrupolar origin. Indeed, the  $\sigma \rightarrow \sigma$  intensity has no magnetic contributions, and we can fit both the  $\sigma \rightarrow \sigma$  and  $\sigma \rightarrow \pi$  intensities using a single scaling factor, which should not be possible with a sizable magnetic contribu-

tion in the  $\sigma \rightarrow \pi$  channel. Such a contribution could originate from an ordered magnetic moment in the bulk, but Mößbauer spectroscopy establishes it unambiguously to be vanishing, or from dipolar order around defects, but this would give broad peaks which are not observed.

While we have no *direct evidence* for a triple- $\vec{q}$  magnetic structure and cannot directly prove the octupolar model, several predictions about the low temperature properties can be investigated. Octupolar order will split the  $\Gamma_8$  CF ground state into a singlet ground state and two excited levels. Inelastic neutron scattering [9] has shown an excitation near 6.5 meV, but the second one is expected to lie below 2 meV, outside the explored energy range. Low temperature specific heat measurements should also show the characteristic signature of the CF spectrum. The integrated entropy from lowest temperatures up to the phase transition should be  $R \ln(4)$ , with a significant contribution from a Schottky anomaly below 8 K. If large single crystals would become available, octupolar order could also be directly observed by neutron diffraction, with a form factor peaking at a finite value of the momentum transfer and reflecting the Fourier transform of the static magnetization density below  $T_0$ .

We thank the ESRF and the beam line staff on ID20 for help with the experiments. Discussions with G. Amoretti and R. Walstedt are gratefully acknowledged.

---

\*Present address: INFN, Dipartimento di Fisica, Università di Parma, I-43100 Parma, Italy.

- [1] D.W. Osborne and E. F. Westrum, Jr., *J. Chem. Phys.* **21**, 1884 (1953).
- [2] R. Caciuffo *et al.*, *Phys. Rev. B* **59**, 13 892 (1999).
- [3] R. Caciuffo *et al.*, *Solid State Commun.* **64**, 149 (1987).
- [4] J. M. Friedt *et al.*, *Phys. Rev. B* **32**, 257 (1985).
- [5] P. Erdös *et al.*, *Physica (Amsterdam)* **102B**, 164 (1980).
- [6] D. Mannix *et al.*, *Phys. Rev. B* **60**, 15 187 (1999).
- [7] W. Kopmann *et al.*, *J. Alloys Compd.* **271–273**, 463 (1998).
- [8] P. Santini and G. Amoretti, *Phys. Rev. Lett.* **85**, 2188 (2000).
- [9] G. Amoretti *et al.*, *J. Phys. Condens. Matter* **4**, 3459 (1992).
- [10] M. v. Zimmermann *et al.*, *Phys. Rev. B* **64**, 195133 (2001).
- [11] F.W. Lipps and H. A. Tolhoek, *Physica (Utrecht)* **20**, 85 (1954).
- [12] D. H. Templeton and L. K. Templeton, *Acta Crystallogr. Sect. A* **41**, 133 (1985).
- [13] V. E. Dmitrienko, *Acta Crystallogr. Sect. A* **39**, 29 (1983).
- [14] V. E. Dmitrienko, *Acta Crystallogr. Sect. A* **40**, 89 (1984).
- [15] Y. Murakami *et al.*, *Phys. Rev. Lett.* **81**, 582 (1998).
- [16] D. F. McMorrow *et al.*, *Phys. Rev. Lett.* **87**, 057201 (2001).
- [17] S. W. Lovesey, *J. Phys. Condens. Matter* **8**, 11009 (1996).